SUPPORTING INFORMATION

Evidence for a Solenoid Phase of Supercoiled DNA

Andrew Dittmore and Keir C. Neuman

Description of open-source Python code in Jupyter Notebook [8]

PHYSICAL PARAMETERS:

- $\beta^{-1} = 4.1$ pN nm is the inverse thermal energy.
- $A = 50$ nm is the persistence length for bending.
- $C = 100$ nm is the persistence length for twisting.
- f is the constant stretching force (in the range 1 to 4.5 pN).
- c is the monovalent salt concentration (in the range 200 to 1000 mM).
- L_0 is the DNA contour length (in the range 1000 to 10000 nm).
- Lk is the excess linking number (restricted to positive values for which the extension $X > 0$).

PHENOMENOLOGICAL CONSTANTS:

- $\mathrm{c}_1 \approx 3$ is a constant used to relate the change in extension energy to the torsional energy savings due to writhe: The torsional energy savings is c_1 times the change in extension energy.
- $\mathrm{c}_2 \approx 54$ when c is in mM and f is in pN. This constant sets the scale for a robust emperical power-law that has not yet been explained by theory. The average torque in buckled DNA increases as $f^{0.72}$ [10] and is assumed inversely proportional to $\ln c$.
- $\mathrm{c}_3 \approx 20$ nm is a constant used in approximating the linking number difference that corresponds to the torque overshoot feature.

CALCULATED QUANTITIES:

- x_{WLC} is the fractional DNA extension given by the Marko-Siggia wormlike chain (WLC) model [20]. We solve the following equation for f by varying x_{WLC} from 0 to 0.999 in increments of 10^{-3}, and then generate $x_{\mathrm{WLC}}(f)$ as an interpolation function.

$$\beta A f = \frac{1}{4}(1 - x_{\mathrm{WLC}})^{-2} - \frac{1}{4} + x_{\mathrm{WLC}} \tag{S1}$$

- C_{eff} is the effective torsional persistence length approximated by additing a term to the Moroz-Nelson formula that takes into account the writhe of a one-turn-per-wave solenoid (eqn. 7). This definition of C_{eff} compares well with the data of Mosconi *et al.* (Fig. 4).

$$C_{\mathrm{eff}}(f) \approx (\frac{1}{C} + \frac{1}{4A\sqrt{\beta A f}})^{-1} - C(1 - x_{\mathrm{WLC}}) \tag{S2}$$

- Γ_u is the torque in unbuckled DNA.

$$\langle \Gamma_u(f, L_0, \mathrm{Lk}) \rangle = 2\pi C_{\mathrm{eff}}(f)/(\beta L_0)\mathrm{Lk} \tag{S3}$$

- X_u is the extension of unbuckled DNA.

$$\langle X_u(f, L_0, \mathrm{Lk}) \rangle \approx L_0 x_{\mathrm{WLC}}(f) - \frac{2(\pi \mathrm{Lk})^2 (C - C_{\mathrm{eff}}(f))}{\mathrm{c}_1 \beta L_0 f} \tag{S4}$$

- Γ_b is the average torque in buckled DNA and assumed constant for $\mathrm{Lk} > \mathrm{Lk}^{\dagger}$.

$$\Gamma_b(f, c) \approx \mathrm{c}_2 f^{0.72} / \ln(c) \tag{S5}$$

- q is the average post-buckling slope (X_b/Lk) in the absence of steps. This definition of q comes from Clauvelin *et al.* [21].

$$q \approx 3\pi\Gamma_b x_{\mathrm{WLC}}/(2f) \tag{S6}$$

- Lk^* is the point at which the post-buckling slope intersects the X_u vs Lk curve. The torque at Lk^* is assumed equal to Γ_b.

$$\mathrm{Lk}^* = \beta L_0 \Gamma_b/(2\pi C_{\mathrm{eff}}) \tag{S7}$$

- X_b is the post-buckling extension in the absence of steps.

$$\langle X_b(f, c, L_0, \mathrm{Lk})\rangle = \langle X_u(f, L_0, \mathrm{Lk}^*)\rangle - q(\mathrm{Lk} - \mathrm{Lk}^*) \tag{S8}$$

- $\mathrm{Lk}^\dagger$ is the buckling transition midpoint at which the unbuckled and buckled states are equal in energy.

$$\mathrm{Lk}^\dagger \approx \mathrm{Lk}^* + \mathrm{c}_3 f/\Gamma_b(f, c) \tag{S9}$$

- P_u is the probability of the unbuckled state.

$$P_u = \left(1 + \exp\left[4\pi^2(\mathrm{Lk}^\dagger - \mathrm{Lk}^*)(\mathrm{Lk} - \mathrm{Lk}^\dagger)C_{\mathrm{eff}}/L_0\right]\right)^{-1} \tag{S10}$$

- P_b is the probability of the buckled state.

$$P_b = 1 - P_u \tag{S11}$$

- X is the approximate DNA extension averaged over fluctuations between states.

$$\langle X(f, c, L_0, \mathrm{Lk})\rangle = P_u\langle X_u\rangle + P_b\langle X_b\rangle \tag{S12}$$

- Γ is the approximate DNA torque averaged over fluctuations between states.

$$\langle \Gamma(f, c, L_0, \mathrm{Lk})\rangle = P_u\langle \Gamma_u\rangle + P_b\langle \Gamma_b\rangle \tag{S13}$$

Many properties of supercoiled DNA can be estimated using this tool. Plots of average supercoiling curves (Fig. S1) and approximate plectoneme geometric parameters (Fig. S2) are shown here as examples [8]. Calculated curves recapitulate experimental data (Figs. S3 and S4), validating this tool for use over the specified limits of the calculation.

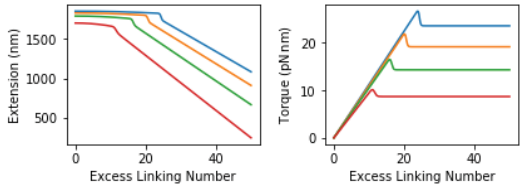

FIG. S1. Average DNA extension and torque vs excess linking number curves calculated using eqns. S12 and S13 at constant forces $f = 4$, 3, 2, and 1 pN. The DNA contour length $L_0 = 2$ μm and the salt concentration $c = 0.5$ M.

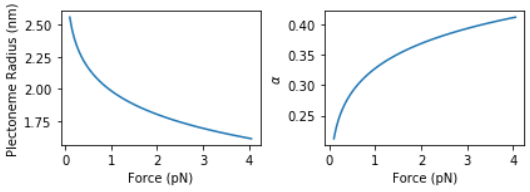

FIG. S2. Average plectoneme radius and ply angle α vs force, estimated at salt concentration $c = 0.5$ M. We numerically solve the equations provided in Clauvelin *et al.* [21] to approximate the plectoneme parameters from our estimates of average torque (eqn. S5) and extension (eqn. S8) of buckled DNA.

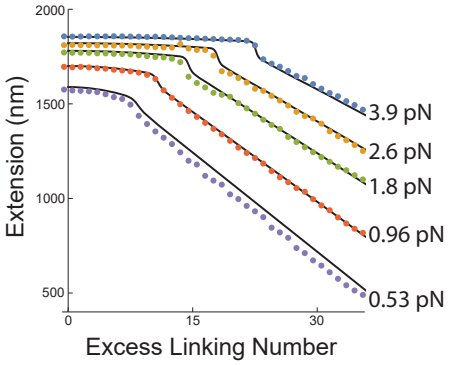

FIG. S3. Overlay of calculated curves (eqn. S12) and average extension vs excess linking number data at $c = 1$ M and various forces, as indicated for each curve. The error bars equal to the standard error of the mean at each data point are smaller than the point size. Measurement points are separated by integer values in Lk. Good agreement is observed within the specified limits of the calculation.

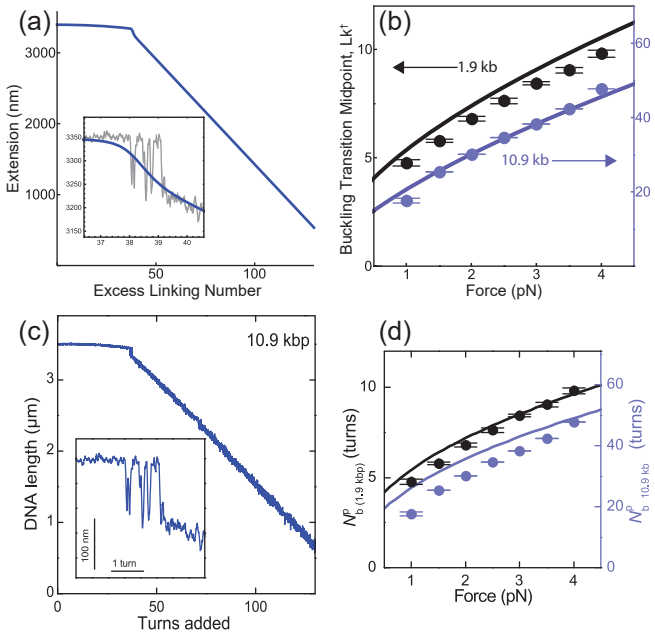

FIG. S4. Calculated curves comparable to data of ref. [27]. (a) Extension vs excess linking number at $c = 320$ mM and $f = 3$ pN for 10.9 kb DNA. Inset shows detail of the buckling transition. For visual comparison, the data curve from Brutzer *et al.* [27] in gray is aligned to our calculated curve (eqn. S12) in blue. (b) Buckling transition midpoint $\mathrm{Lk}^\dagger$ vs force at $c = 320$ mM and two different DNA lengths. Left scale: 1.9 kb. Right scale: 10.9 kb. The solid curves are our calculations (eqn. S9) and the data points are from Brutzer *et al.* [27]. (c-d) Figures from ref. [27] (reproduced with permission) corresponding to panels a and b.

Experimental methods

We prepared ≈6 kb DNA molecules for testing in magnetic tweezers using established methods [2,28]. Each DNA molecule of contour length $L_0 \approx 2$ μm was isolated and torsionally constrained between an antibody-coated glass surface and a ~ 1 μm streptavidin-coated paramagnetic bead (Dynal) using multiple biotin or digoxigenin moieties at either extremity. A magnetic field gradient, controlled by the proximity of permanent magnets, pulled the bead upward and extended the DNA. At constant force, magnet rotation synchronously rotated the bead, permitting control over DNA linking number. We performed DNA supercoiling measurements at varying concentrations of NaCl in 10 mM Tris buffer, pH 7.5 at room temperature. To observe steps (Fig. 1), we collected DNA extension vs excess linking number data using the radial intensity pattern of bead images [2,28], magnified at 125 nm per pixel on a CCD camera with 5 ms exposure time. We collected 1000 data points at each value of constant excess linking number Lk, and discarded 100 intervening points during which we rotated the bead in 0.1 turn increments. For data visualization, we approximated a continuous supercoiling curve by plotting successive points at a separation of 10^{-4} in Lk. The

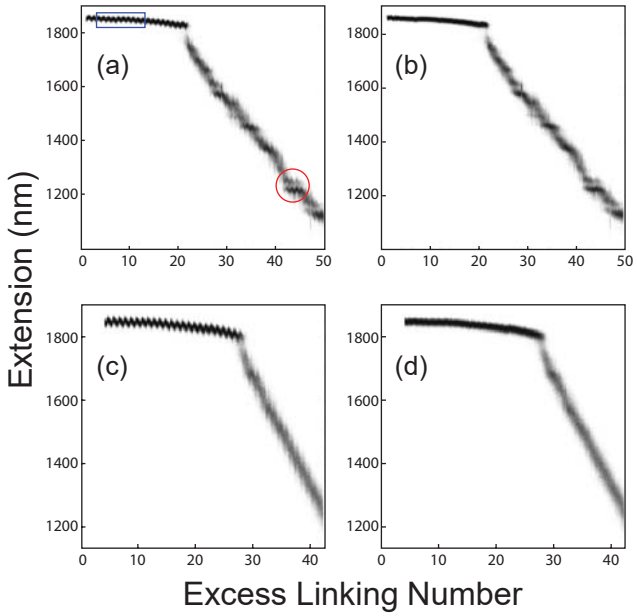

FIG. S5. Correcting errors due to bead rotation. (a) Raw data collected at 3.6 pN force in 25 mM Tris buffer, pH 7.5 with 100 mM potassium glutamate and 10 mM $MgCl_2$. Blue box: region of ten bead rotations showing the extension measurement error. Red circle: errors due to rotation are present within a plectoneme lengthening step, showing that rotation errors are distinct from steps. (b) Data from part a after correction. (c) Raw data collected at 3.6 pN force in 10 mM Tris buffer, pH 7.5 with 100 mM NaCl. (d) Data from part c after correction.

signal of discontinuous plectoneme lengthening steps is measurable at relatively high force ($f > 1$ pN) and high ionic strength ($c > 100$ mM). Here, our measurements and model pertain to monovalent salt solutions; to encourage further experimental studies, we note that a small concentration of divalent ions has a strong influence on the discontinuous supercoiling of torsionally buckled DNA (Fig. S5).

Correction for measurement errors due to bead rotation

Subturn rotations of the bead cause slight errors in the apparent DNA extension that repeat modulo 1 turn. These ∼10 nm errors are distinctly different than our observation of plectonmeme lengthening steps, which remain after removing bead rotation errors from the extension vs excess linking number curve (Fig. S5). We did this using the following procedure:

1. Select a region (typically spanning ten turns) from the shallow region of the curve ($Lk < Lk^{\dagger}$) (Fig. S5a, blue box).
2. Fit a line to data in this region (Fig. S6a). A line over ten turns is a good local approximation of the underlying parabolic shape.
3. Subtract the fit line from the data. What remains is the error of repeating oscillations that is different for each bead (Fig. S6b).
4. Collect all points with the same Lk values (modulo 1) and calculate their means. This gives a representative wavelet signal over one bead rotation (Fig. S6c).
5. Subtract the repeating wavelet signal across the extension vs excess linking number curve to correct for bead rotation errors (Fig. S5b).

Experimental estimation of step size and ΔLk between steps

Starting with extension vs excess linking number data (Fig. S7a), we used the distances between neighboring peaks in the histogram of extension values to estimate the average step size between buckled states, and used the positions of local minima to define thresholds separating states (Fig. 7b). We then counted the number of points within neighboring states (above or below threshold) in non-overlapping 1000-point intervals corresponding to constant Lk increments (Fig. S7c). Finally, we fit the logarithm of the ratio of points to a line crossing zero at the transition midpoint, and estimated ΔLk between steps as the average difference between transition midpoints (Fig. S7d).

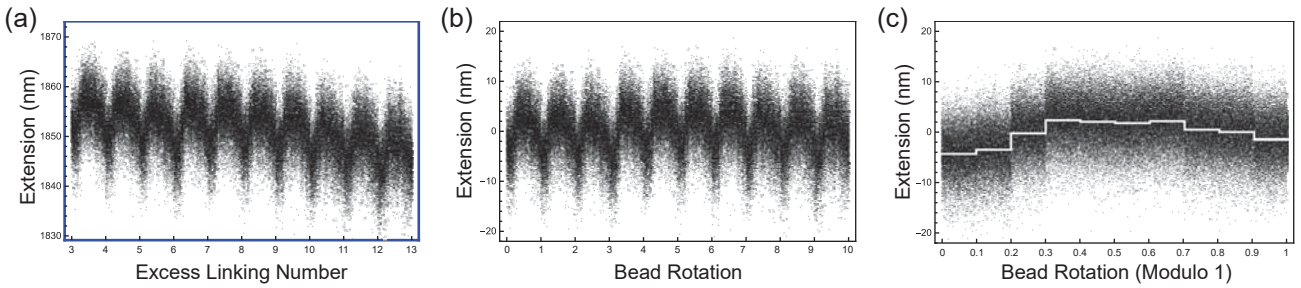

FIG. S6. Process for correcting errors due to bead rotation. (a) Data in selected region from Fig. S5a. (b) Data in panel a after line subtraction. (c) Data in panel b modulo 1 bead rotation. The white line is the mean extension error at each 0.1 turn increment of bead rotation and can be removed because it repeats at each integer multiple of excess linking number, Lk. The rotation error is different for each bead.

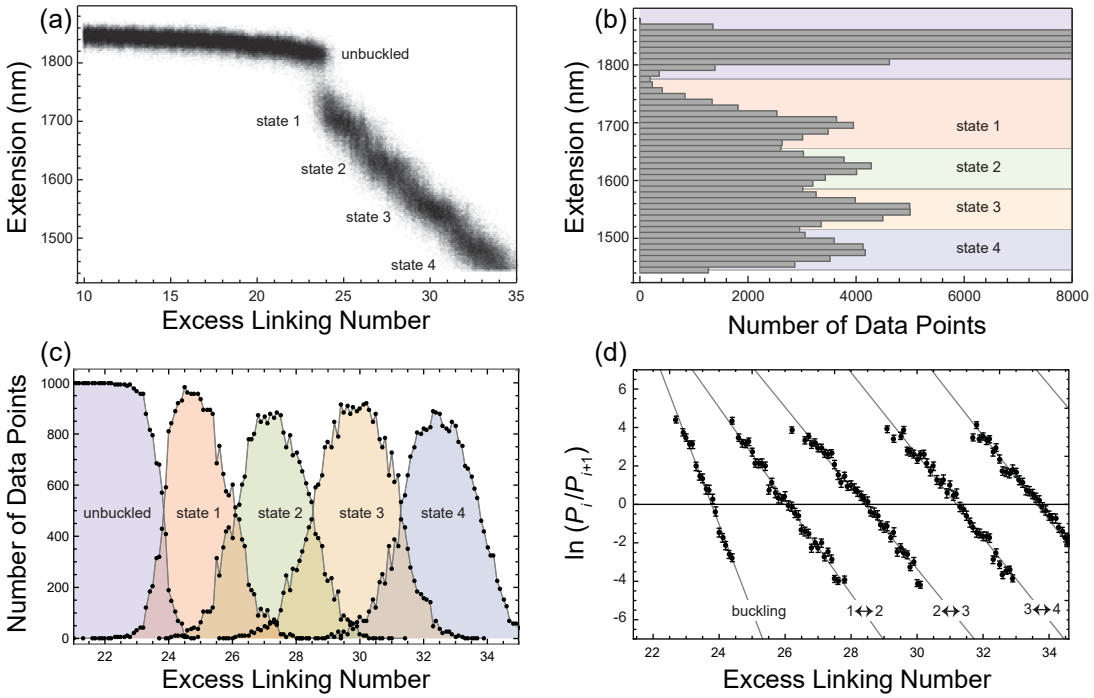

FIG. S7. Process for determining step size and ΔLk between steps. (a) Data from Fig. 1a including points populating the unbuckled state and four discrete buckled states. (b) States are separable by local minima in the histogram of extension values. Experimental values of step size in Fig. 3 are the average peak-to-peak extension difference between neighboring buckled states. (c) The number of data points in each state as a function of excess linking number, Lk. (d) The logarithm of the probability ratio, P_i/P_{i+1} as a function of Lk, through the series of equilibrium transitions between buckled states i and $i+1$. (These are preceded by the buckling transition with probabilities P_u of the unbuckled state and P_b of the first buckled state.) Error bars represent the standard error of proportion based on binomial sampling. A linear fit crosses zero at each transition midpoint. Experimental values of ΔLk between steps in Fig. 3 are the average separation between neighboring transition midpoints after buckling.

Calculation of C_{eff}

Winding causes an initially unstraight elastic rod to develop a one-turn-per-wave solenoid [19]. We assume that this general physical phenomenon observed in macroscopic elastic rods also occurs microscopically in overwound DNA, and posit that a one-turn-per-wave solenoid resides in the background of an overall fluctuating DNA structure. Since twist-reducing fluctuations are already taken account in the Moroz-Nelson theory [9], we seek an estimate of the writhe-per-link associated with a static background solenoid as would occur in the absence of modifying fluctuations. For a regular one-turn-per-wave solenoid, the total torsion (Lk) about the central axis is greater than the twist (Tw) along the body of the rod because some of the torsion is in writhe (Wr) which reduces twist. From simple geometry, Tw equals the number of waves Lk times the sine of the helix opening angle, which is equivalent to the ratio of the

rod length component along the central axis to the total rod length; in other words, the twist-per-link is equal to the height-to-contour-length ratio. From $\mathrm{Lk} = \mathrm{Tw} + \mathrm{Wr}$, the writhe is $\mathrm{Wr} = \mathrm{Lk}(1 - \mathrm{Tw}/\mathrm{Lk})$. Furthermore, in the absence of twist-reducing fluctuations (which also reduce height), the height-to-contour-length ratio of a DNA molecule is equal to the fractional DNA extension, x_{WLC}, as given by the Marko-Siggia wormlike chain model [20]. Therefore, the writhe-per-link associated with the background solenoid is simply $1 - x_{\mathrm{WLC}}$ [11]. Under the assumption that the solenoid plus fluctuation components of writhe are linearly additive, we propose the following augmentation of the Moroz-Nelson formula for the effective torsional persistence length, C_{eff} (eqn. 7 or eqn. S2), in which the first term is the Moroz-Nelson formula and the second term accounts for writhe in a static one-turn-per-wave solenoid.

$$C_{\mathrm{eff}}(f) \approx \left(\frac{1}{C} + \frac{1}{4A\sqrt{\beta A f}}\right)^{-1} - C(1 - x_{\mathrm{WLC}}(f)).$$

Fig. 4 demonstrates the success of this formula, supporting our conjecture that a one-turn-per-wave solenoid resides in the background structure of overwound DNA.

Calculation of step size and ΔLk between steps

Given a background one-turn-per-wave solenoid (discussed above), twist-reducing fluctuations are expected to further modify writhed DNA structure and compact the solenoid, whose wavelength can be estimated as X_u/Lk ($\mathrm{Lk} < \mathrm{Lk}^\dagger$) or $X_u/\mathrm{Lk}^\dagger$ ($\mathrm{Lk} \geq \mathrm{Lk}^\dagger$). Since overwound DNA buckles at $\mathrm{Lk}^\dagger$, $X_u/\mathrm{Lk}^\dagger$ provides a rough estimate of the step size (Fig. 2). A more refined estimate takes into account the length scale of bending fluctuations reducing the estimated step size. Our fluctuating solenoid model predicts

$$(\text{step size}) \approx \langle X_u(f, L_0, \mathrm{Lk}^\dagger)\rangle/\mathrm{Lk}^\dagger - 2\sqrt{A/(\beta f)}. \tag{S14}$$

The change in linking number between steps is related to the step size through the slope, q, and is estimated as

$$(\Delta\mathrm{Lk} \text{ between steps}) = (\text{step size})/q. \tag{S15}$$

We calculate both the step size and ΔLk between steps using eqns. S4, S6, and S9. These estimates compare favorably with the data presented in Fig. 3 without fitting, further supporting our model of a fluctuating solenoid in the unbuckled region of overwound DNA.